



# Nearshore Seafloor Depositions and Deformations at Paleo-Glacier Active Area revealed from side scan sonar data, case study from Horseshoe Island, Western Antarctica.

Denizhan Vardar<sup>1</sup>, Mehmet Korhan Erturaç<sup>2</sup>, Orkan Özcan<sup>3</sup>, Cem Gazioğlu<sup>4</sup>

1. Istanbul University, Institute of Marine Sciences and Management, Marine Geology and Geophysics Department

2. Gebze Technical University, Institute of Earth and Marine Sciences

3. Istanbul Technical University, Eurasia Institute of Earth Sciences

4. Istanbul University, Institute of Marine Sciences and Management, Marine Environment Department+

*Correspondence to:* Denizhan Vardar (denizhan@istanbul.edu.tr)

5 **Abstract.** The variety of geophysical imaging methods, such as shallow-acoustic profiling, multi-beam swath bathymetry, and side scan sonar, has made it possible to recognize and understand submerged glacial landforms on and below the seafloor of historically glaciated continental edges. By examining these landforms, one can learn more about the dynamics of paleo ice sheets and the processes by which ice sheets move, erode, and deposit sediment. In order to evaluate model projections of the future responses of the Greenland and Antarctic ice sheets to climate change, it is equally crucial to comprehend previous rates of change. In order to accomplish this, the video ground-truthing and side scan sonar data, which are the initial dataset for the study area, were used to map the nearshore deformations and deposition features of Western Horseshoe Island, Western Antarctica. The morphological and erosional boundaries indicate that streams of melting ice have affected the seafloor, especially below 10 meters, in the recent past, forming glacial marine phases and ice-margin. Nonetheless, a limited area also revealed subglacial seafloor features, such a paleolake, and paleoshoreline morphology, suggesting the presence of a two-phase mechanism in the study area. Meltwater streams and ice flow directions in the research region generally trend southward, with the island's southernmost portion being deeper than its westernmost component.

## 1 Introduction

25 During the Quaternary, the geomorphology of land and continental shelf in mid-high latitudes is dominated by advancing and retreating glaciers during the glacial-interglacial cycles especially during the stadial periods (Svendsen et al. 1999; Dyke et al. 2002). The subglacial, ice-margin, and glacialmarine landforms were created as a result of the spread and recession of ice along these boundaries. While surficial processes and human activities have interrupted the record of glacial activity on land, glacial landforms are frequently well conserved in the marine environment and can be observed in continental shelves, slopes, and basins (Solheim et al. 1991; Shipp et al. 1999; Dowdeswell et al. 2002; Ottesen et al. 2005; Larter et al. 2012).

30 The proliferation of studies on submarine glacial landforms has been facilitated by advancement in geophysical imaging techniques. Initially, single-beam echo sounders were used to study seafloor morphology (Damuth 1978). Later



advancements in side-scan sonar and multi-beam echo sounders enabled large-scale seafloor mapping, along with the identification of ancient landforms beneath the seafloor using shallow acoustic and two-dimensional seismic reflection profiles (Dowdeswell et al. 2006).

35 The Side Scan Sonar (SSS) system is an efficient acoustic technique that offers high-resolution imaging of the seafloor with a wide sweep range and nearly photographic quality. The SSS system is highly beneficial in classifying seafloor sediment types (such as sand, clay, gravel, mud, etc.) based on backscattering strength (Richardson et al., 2001; Briggs et al., 2001; Goff et al., 2004; Ferrini and Flood, 2006; Buscombe, 2017) as well as in mapping geological structures (such as outcrops, faults, etc.) that cause acoustic differentiation on the seafloor. Low backscatter intensity indicates finer sediments with high  
40 porosity, low density, and sound velocity. On the other hand, higher backscatter intensity is more likely to occur from coarser sediments with lower porosity since they increase density and velocity. Regarding the impact of particle size on backscatter intensity, there are several significant cautions to take into account. For example, muddy sediments may contain near-surface gas, which could increase backscatter intensity (Borgeld et al., 1999, Fonseca et al., 2002). Similar to this, subsurface changes in impedance contrast can result in high acoustic backscatter intensity when fine-grained surface  
45 sediments sit above coarser beneath sediment layers. High backscattering intensity in fine-grained sediments can also result from the existence of subsurface inhomogeneity brought on by bioturbation (Urgeles et al., 2002). Seafloor surface roughness is an important variable to consider in terms of high-frequency acoustic backscattering intensity and has been studied by many researchers (Stewart et al., 1994; Briggs et al., 2001; Richardson et al., 2001). The effects of roughness on backscattering intensity vary depending on the type, magnitude and direction of the roughness, as well as the frequency of  
50 the acoustic signal.

Detecting debris and deformations on the seafloor is another important use for SSS (Barnhardt et al., 1998; Collier and Brown, 2005; Grindlay, 2009). Techniques for acoustic seafloor characterization have proven to be highly helpful in imaging the characteristics of the seafloor and providing crucial data for studies in marine geology, hydrography, marine engineering, environmental sciences, and other fields. When compared to traditional seabed sampling techniques (such as grab and core  
55 sample; Bull et al., 1998), high-resolution seafloor imaging with large swath widths has the advantage of saving survey time and lowering expenses. However, the various reflections from the seafloor should be corrected using conventional means (such grab sampling - video captures) or earlier research if enabled, particularly for the sediment distribution mapping investigations.

Reconstructing the structure and dynamics of past glaciers and ice sheets is made possible by the analysis of submarine  
60 glacier landforms. According to Stokes et al. (2016), defining historical changes provides crucial information for modeling the future behavior of the Greenland and Antarctic ice sheets in response to climate change. Locating past ice streams—relatively narrow corridors of fast-moving ice within slower-moving areas of an ice sheet—is a major goal in ice sheet reconstruction (Bentley 1987; Dowdeswell and Siegert 1999; Whillans et al. 2001). Ice streams have the ability to cause



abrupt climate change by rapidly delivering ice and meltwater to the marine ice-sheet margin (MacAyeal 1993; Clark 1994)  
65 and also respond dynamically to perturbations over short, sub-decadal time-scales (Anandakrishnan and Alley 1997; Joughin  
et al. 2003).

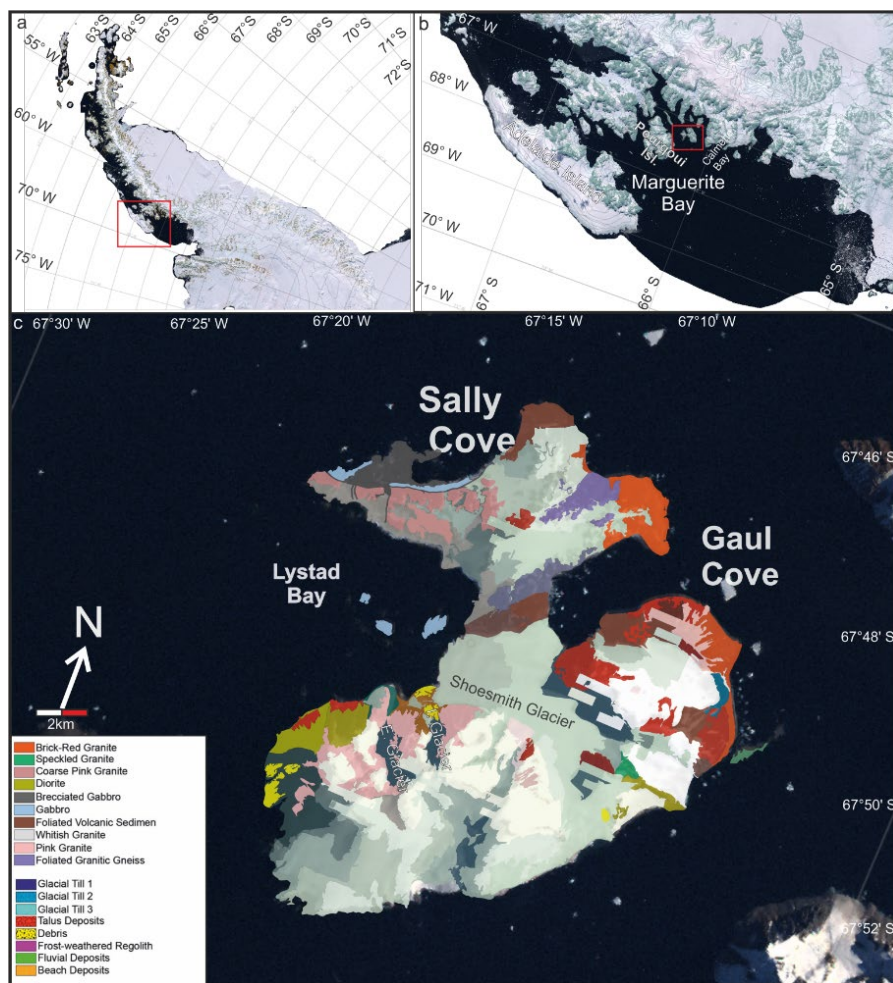
The formation of deep bathymetric depressions known as cross-shelf troughs, surrounded by shallower banks, is caused by  
fast flowing ice streams that erode the continental shelf (Vorren and Laberg 1997; Dowdeswell and Siegert 1999; Batchelor  
and Dowdeswell 2014). The term "cross-shelf troughs" refers to groups of glacial features that show rapid, ice-streaming  
70 flow. These features include pervasively deformed till and elongate, streamlined landforms produced by subglacial processes  
(Stokes and Clark 2001; Shipp et al. 1999; Ó Cofaigh et al. 2002; Dowdeswell et al. 2004). Progradation of the sedimentary  
depocentres, called trough-mouth fans, generally develop on the continental slope seaward of cross-shelf troughs that have  
experienced high rates of sediment delivery to the shelf edge over successive full-glacial periods (Dowdeswell et al. 1996;  
Elverhøi et al. 1998; Dowdeswell and Siegert 1999). The glacial landforms preserved on the intervening shallower banks are  
75 characteristic features of the slower-flowing ice (Ottesen and Dowdeswell 2009).

Large-scale studies of deep and relatively shallow seafloor features are well-researched in glacially active marine areas;  
however, smaller-scale studies that examine shallow marine areas and focus on structures affecting nearshore areas are  
extremely rare, presumably because of the challenging conditions for data collection. However, hydrodynamic factors in  
nearshore areas are highly variable and have significant impacts on the seafloor. Therefore, these investigations are crucial  
80 for identifying nearshore interactions and for informing future climate estimates.

This study presents the initial data set aiming to describe the seafloor properties in nearshore areas (0-50 m) at the western  
part of Horseshoe Island (Marguarite Bay, West Antarctic Peninsula, Figure 1). The primary goal is to determine nearshore  
interactions and their consequences on sediment distribution in glacially active areas. Side-scan sonar data were collected,  
and seafloor classification was made based on changes in reflection amplitude. Movement directions in glacier and/or glacier  
85 boundary active areas were identified, and an underwater drone was operated to capture images for ground verification at  
designated locations.

## 1.1 Study Area

The study area (offshore Western Horseshoe Island) is located in the south-central region of the Antarctic Peninsula, within  
the Marguerite Bay archipelago (Fig. 1a–b). About 20 ka ago, an ice sheet covering the bay extended to the continental slope  
90 (Bentley et al., 2011). There were two significant phases in the deglaciation process, occurring shortly after 14.2 ka and 10.6  
ka, leading to the disappearance of the icesheet and the flooding of the inner section of the bay (Ó Cofaigh et al., 2008). By  
9.5 ka, the marine area was free of ice sheets (Çiner et al., 2019). These significant climatic events had a considerable impact  
on seafloor of the bay.



95

Figure 1. The location map of the study area a) Western Part of Antarctica Continent, b) Map shows Marguerite Bay and Horseshoe Island c) Geology and geomorphology map of the study area (Matthews, 1983 and Yıldırım, 2020; abbreviations of E: Erinç, I: Izbirak)

## 1.2 Onshore Geology and Morphology

100 Horseshoe Island, located in the Marguerite Bay (Figure 1b), is the third largest island in the archipelago. Approximately sixty-six percent of its 60 km<sup>2</sup> area is covered by glaciers or semi-perennial ice and snow. Mount Breaker (879 m a.s.l.) and Mount Searle (537 m a.s.l.) are the island's highest peaks. In the center of the island lies a glacier-free saddle (80 m a.s.l.) forming a plateau (500 x 750 m in dimension) that connects its northern and southern sectors. There are five freshwater lakes situated on the plateau surface. Additionally, three glaciers -Shoemith, Erinç, and Izbirak- covers the most land on the

105 southern part of the island. The study area experiences a cold and dry marine climate (Ochyra, Lewis, Smith, & Bednarek-Ochyra, 2008).



Horseshoe Island's bedrock primarily consists of mafic igneous rocks such as gabbro and undifferentiated volcanic rocks, as well as felsic igneous rocks like white, pink, brick-red, and mottled granites and diorite. A dense network of basaltic dykes cut through this basement forming distinct linear differential erosional morphology (Matthews, 1983, Figure 1c). Quaternary deposits on the island, as described by Yıldırım (2020), include frost-shattered rocks and regoliths, soil within moraines, erratic blocks on bedrock, debris mats on glaciers, talus deposits along mountain fronts and cliffs, beach deposits, and fluvial deposits of braided streams.

## 2 Material and Method

The acoustic reflection dataset was acquired using the DeepVision DE3468D Dual CHIRP Digital 340/680 kHz SSS system in February 2024. To ensure a high-quality dataset considering the features of seafloor morphology; we utilized a frequency of 340 kHz frequency and a baud-rate of 128.000. With a wavelength of approximately 4 mm, the theoretically minimum along-track resolution is about 1.5 cm (calculated assuming a horizontal beam width of 0.9°), and the swath-range is 150 m (totaling 300 m). The following basic data processes were applied to the SSS data:

Pre-processing involves converting the recording format to the program format. Main processing includes radiometric calibration and mosaic processes. Post-processing aims to increase the quality by eliminating noise.

Seafloor sediment identification was conducted following the criteria outlined by Barnhardt et al. (1998). The definitions of the main units' reflection are provided in [Table 1](#).

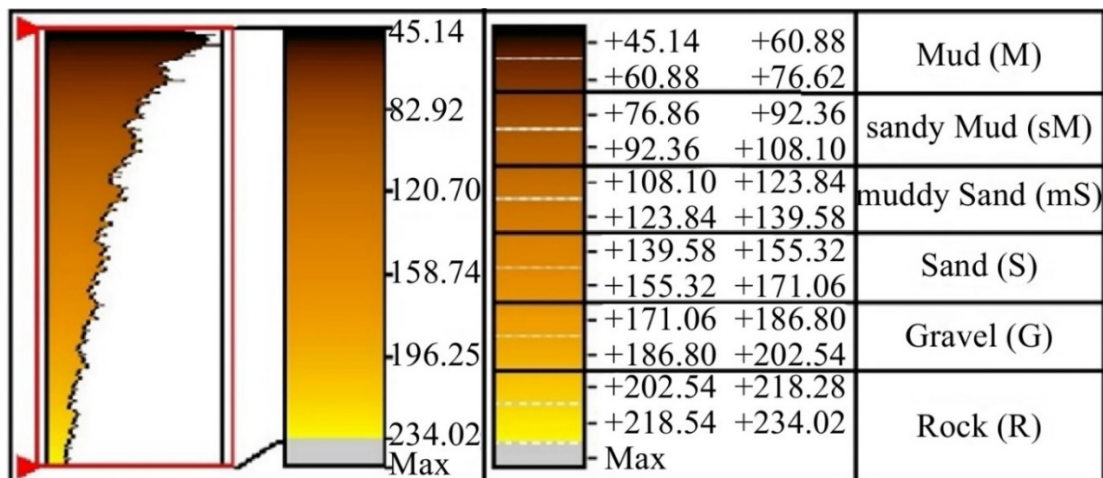
**Table 1.** Acoustic reflection intensity and the outcrop features of the seafloor formations, Barnhardt et al. (1998)

Map Unit	Acoustic Intensity	Reflection	Outcrops Features
Mud (M)	Weak		Smooth flat
sandy Mud (sM)	Weak		Smooth flat
muddy Sand (mS)	Medium		Smooth flat
Sand(S)	Medium		Smooth flat
Gravel (G)	Strong		Low relief often covered with ripples or boulders
Rock (R)	Strong		High relief, fractures common

Furthermore, the sediment unit influences the intensity values of the acoustic signals generated by the side-scan sonar, which reflect from the seabed and return to the receiver. Each of these color-coded value ranges represents a distinct sediment unit (Fig. 2). The SonarWiz program provided these unit ranges (Pratomo et al., 2018). The acoustic data collected was used to



calculate these reflections and amplitude values. Subsequently, the boundaries indicating their overlap and correlation with earlier research were mapped.



130 Figure 2. Acoustic classification according to backscattering intensity of the seafloor formations (Ozgan et al. 2024)

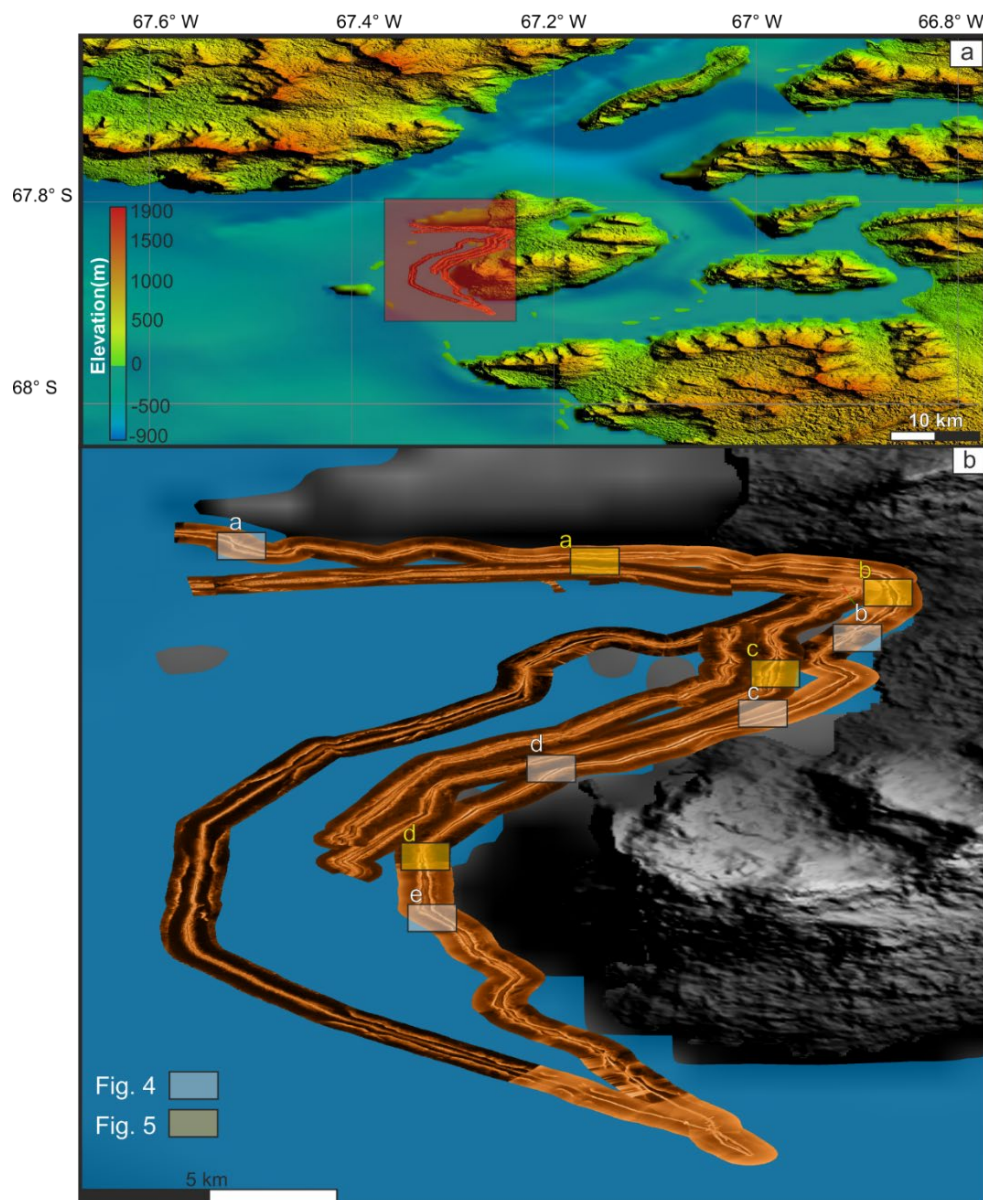
The color scale for the seafloor classification varies from extremely dark brown to light brown according to the reflection intensities (strong to weak). Since color darkness and reflection intensity are inversely correlated, "Mud (M)" is the seafloor deposit with the darkest color and the lowest reflection density. The sediment sequence continues as "sandy Mud (sM), muddy Sand (mS), Sand (S), and Gravel (G)," depending on the decline in reflection density and the progressive lightening

135 of the hue. "Rock (R)" is the seafloor formation with the lightest hue (light brown) and the strongest reflection intensity. (Table 1, Figure 2)

### 3 Results

Approximately 80 km of side scan sonar data were collected from the study area (Fig 3), covering an area of approximately 16 km<sup>2</sup> with an average total swath range of 200 m within the Lystad Bay and reaching to the southwestern part of the island. The air temperature was -4°, seawater -1°, with an average wave height of 0.5 meters. A 3 m long zodiac boat was used, with a fixed average boat speed of 1-1.5 knots. Acoustic data collection in the study area was conducted in accordance with coastal morphology, with instantaneous route changes made when the sea surface was covered with ice. In this context, the erosional and morphological boundaries and the distribution of sediments according to grain size were revealed in the study area. The locations of the reflection examples in the study area presented in Figs 4 and 5 are shown in Fig 3.





145

Figure 3a. Side scan sonar profiles routes (Topography data is Aster V2 Data, Bathymetry data is ETOPO 1 Data) b) Zoomed view of the red square shows the locations of the sonogram examples given in Figs 4 and 5

### 3.1 Erosional and Morphological Boundary Reflections in the Study Area

The studied area is subject to significant erosional forces, and the relationship between these forces and morphological structures may be discerned in the acoustic recordings. The morphological and erosional borders for this study are presented

150



using the greyscale color band on sonogram records because it is helpful in discerning the boundaries based on high-contrast features (Fig. 4).

155 Westerly erosions were observed on the close shore, while southerly erosional boundaries were noted in the northwest portion of the research region (Fig. 4a). Furthermore, these erosions considerably overprinted the base morphological structures (Fig. 4). The morphological boundaries and erosion directions in the north center of the research area point to east to west and southeast, respectively (Fig 4b). Despite the observation of iceberg plough mark reflections in the west center of the island, the research region has a restricted number of these marks (Fig. 4c). Further south, the direction boundaries are about WSW due to deeper and wider deformations on the sea floor morphology caused by erosional impacts (Figs. 4d and e).  
160 a steep gradient. Seafloors deeper than -140 m are observed towards the south of the island, towards the offshore area.

### 3.2 Acoustic definition of the seafloor deposition units

Enormous rock blocks are visible on the nearby coastlines in the northwest section of the bay. These rocks gradually decrease in size as you move eastward in the nearshore regions. Their distribution is largely consistent with the shape of the shore, and these reflections were identified as moraines. Additionally, evidence of a sedimentary ridge facing west was  
165 observed in this region (Fig 5a). Near this ridge, low amplitude reflection is interpreted as the beginning of mud and extends across a large area to the west. However, some medium to strong reflections were determined on this unit (Fig 5a). Large rock blocks are dispersed throughout the easternmost portion of the gulf, along with a morphological boundary described as a grounding zone wedge, and sedimentary units exhibiting westward flow were noted (Fig 5b).

An area of low amplitude deposition is found in a limited area, characterized as a paleo-lake, at the Lystad Bay, located  
170 between the coast and the small islands (Fig 5c). To the west of this area, there are two paleo-coastal boundaries at different depths. Moraine deposits oriented towards the center were identified both to the west of the island and to the east of the small islands. Sediment reflections indicating sediment flux towards the center were also observed in these areas.

The erosion in this location becomes more profound as one moves southward on the island. Medium-low amplitude sedimentary reflections were observed, and the density of moraine deposits decreases (Fig 5d). Medium-high amplitude  
175 reflections are dispersed over a large area on the western edge of this location. Abrupt, steep changes have begun from the bottom to the island's far south and west.



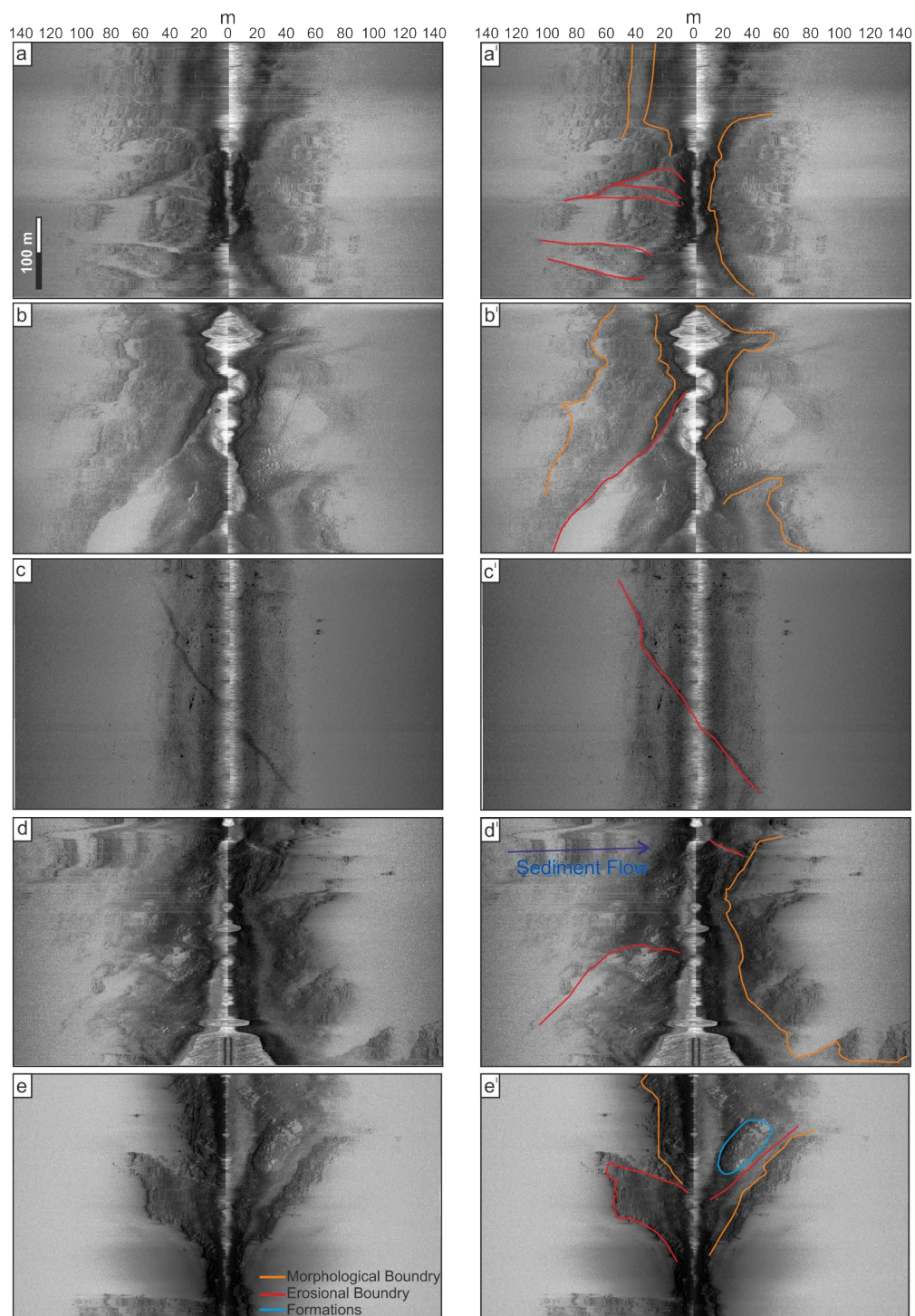
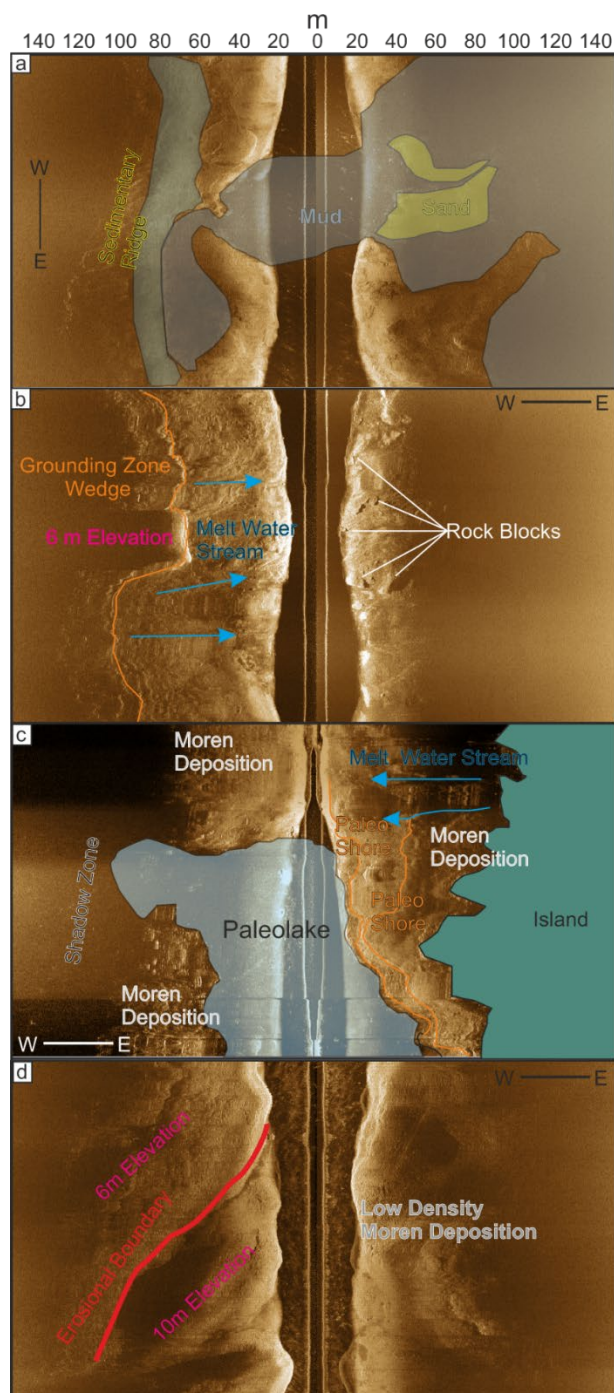


Figure 4. Interpreted and non-interpreted sonogram examples that show erosional and morphological boundaries at the study area. See Fig 3b for the locations



180

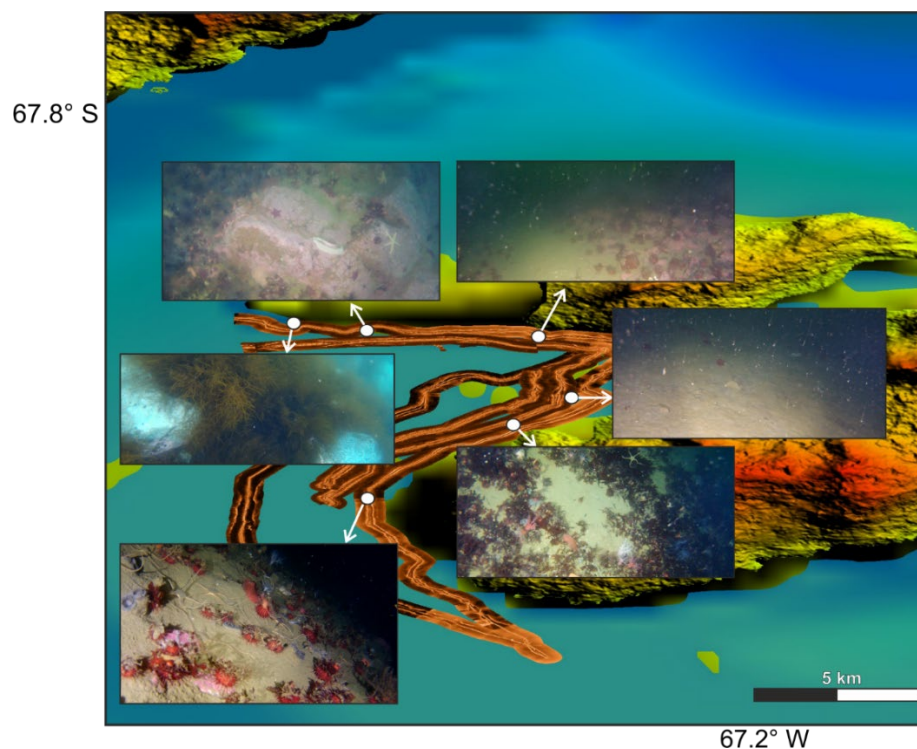
Figure 5. Sonogram examples that show the deposition characters, morphological features and stream directions according to the sediment flow. See Fig 3b for the locations



### 3.3 Ground trothing of reflections via video captures

For ground trothing, the QYSEA V6 underwater drone was used at six station. Despite the negative effects of high current velocity, high primary bioproduction in saltwater, and cold water reducing the battery performance, high-quality captures were nevertheless achieved by approaching the seafloor closely.

In the near coast areas approximately 3-5 meter depth in the northwestern part of the study area, large white granite blocks are observed. To the west, at approximately 5-10 meter depth, pink granite blocks are observed, and the fine-grained sediments begin to cover this formation (Fig 6). Moving towards the inner north side of the study area, the size of the pink granite blocks decreases, and at the depths of 15-20 meters, this formation ends, with small-grained sediments covering the seabed. In the southern part of the study area, at depths of approximately 15-25 meters, small-grained sediments cover the entire area, with dispersed and rare small rocks. Deeper than 25 meters in the southern parts of the study area, the seafloor is covered by fine-grained sediments (Fig. 6).



195 Figure 6. Video captures for ground trothing for the study area

## 4 Discussion

The marine area in the western part of Horseshoe Island, including Lystad Bay, has been extensively surveyed with a side-scan sonar system, providing detailed information up to a water depth of 50 meters. This survey has allowed for the mapping



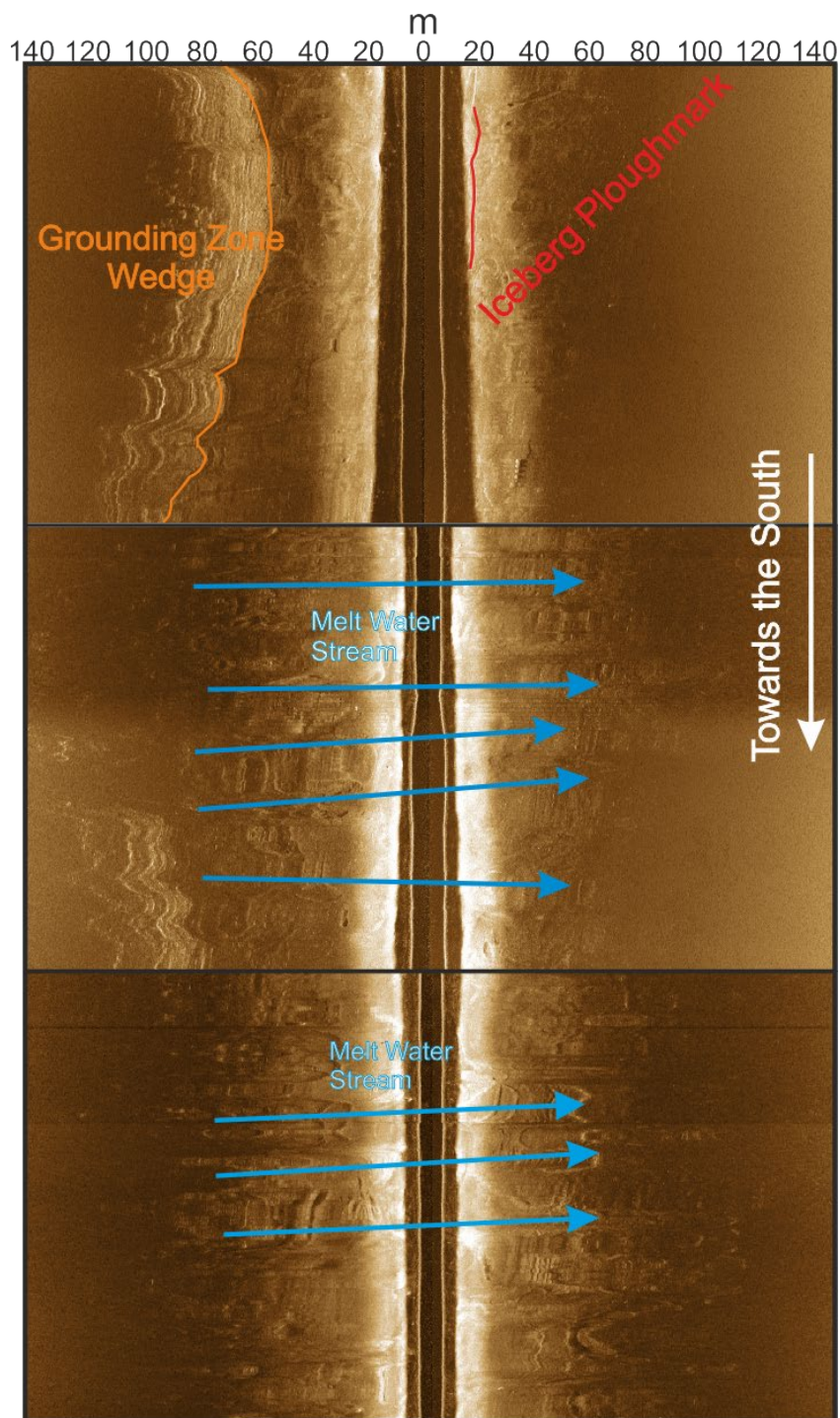


of sediment grain sizes, erosional boundaries, depositional areas, and glacial or glacier-induced flow directions in the study  
200 area, based on acoustic data. These findings and datasets represent the first comprehensive study of the area, as studies  
focusing on the nearshore in glacier-active areas are rare worldwide. Typically, marine studies tend to focus on larger-scale  
assessments and deeper areas, while studies in nearshore regions are limited (Solheim et al., 1991; Shipp et al., 1999;  
Dowdeswell et al., 2002; Ottesen et al., 2005; Larter et al., 2012; Bart et al., 2017; Danielson and Bart, 2019; Danielson and  
Bart, 2024). Despite this, the seafloor structures formed by ice mechanisms in nearshore areas remain relatively undefined.

205 However, interpretations have been made based on well-defined main phase systems (Batchelor et al. 2018)

A sidescan sonar system was used to conduct a comprehensive investigation of the seafloor in the marine region, including  
Lystad Bay on the western part of Horseshoe Island, reaching down to a depth of 50 meters. The acoustic data-set was  
employed various features such as sediment grain sizes, erosional boundaries and depositional areas, glacial and glacier-  
induced flow directions within the research area. Studies focusing on the nearshore in glacier-active locations are extremely  
210 rare worldwide, making our findings and datasets the first for this particular research area. Typically, marine studies tend to  
focus on larger-scale assessments and relatively deeper areas (Solheim et al. 1991; Shipp et al. 1999; Dowdeswell et al.  
2002; Ottesen et al. 2005; Larter et al. 2012, Bart et al, 2017, Danielson and Bart, 2019; Danielson and Bart, 2024). In this  
context, the seafloor structures formed by ice mechanism identified in nearshore areas remain relatively undefined. However,  
interpretations have been made based on well-defined main phase systems (Batchelor et al. 2018), interpretations were made  
215 accordingly.

The data collected in the research area revealed the presence of the grounding zone wedge, a morphological boundary that  
represents the ice-margin phase of the ice-sheet glacier. Dense moraine stacks are another example of this morphological  
feature. Additionally, features originating from meltwater streams, often referred to as plumes, were observed immediately  
beyond the grounding zone wedge, indicating the glacial marine phase (Fig. 7). Furthermore, a limited number of iceberg  
220 ploughmark erosions were also detected within the research region. Flow-induced sediment deposits flow and/or glacial  
movement-induced erosional structures provide valuable information about past glacial movements. Erosional features align  
with the direction of upstream flow, while certain sedimentary and morphological units, such as lateral moraines, run parallel  
to the flow direction.



225 Figure 7. An example for the general ice-flow relation in the study area





As additional data, the multi-beam bathymetry map published in Tükenmez et al. 2022 was integrated into the flow map (Fig 8). According to the map, there is a westward flow in the coastal areas near the northwest of the Lystad Bay. This flow is supported by the formation of E-W oriented sedimentary ridges and westward erosional boundaries. Moving towards the east, the directions of erosional boundaries begin to turn towards the south, and the morphological boundaries align parallel to these orientations. The common west to east erosional orientations in the westernmost side scan lines with multi-beam bathymetry data start from a south-easterly direction and continue with an increasing slope to the south. In the western parts of Horseshoe Island, the orientations are concentrated as west and southwest. In the central southern parts of the island, both the depths increase towards the south and the seafloor erosion depths increase towards the west. In these areas, compared to the northern and central parts of the island, there is an orientation towards the main flow passing through the center of the gulf from east and west. As they descend from the central part of the island towards the south, this flow is still being fed from the west, but in the eastern area, it has created important erosion areas with its flow force and continued its southward flow. In the south of the island, the seafloor went out of the swath range of 150 m, and although the southern lines were discarded for a while, the seafloor was not observed in the sonogram records on the return and return lines. In the south of the island, the seabed has moved out of the swath range of 150 m, and although the southern lines were continued for a while, the seabed was not observed in the sonogram records and also on the return profiles. Therefore, considering the erosion and flow mechanisms of the island, it is concluded that this is an important glacially influenced deformation area (Fig 8).

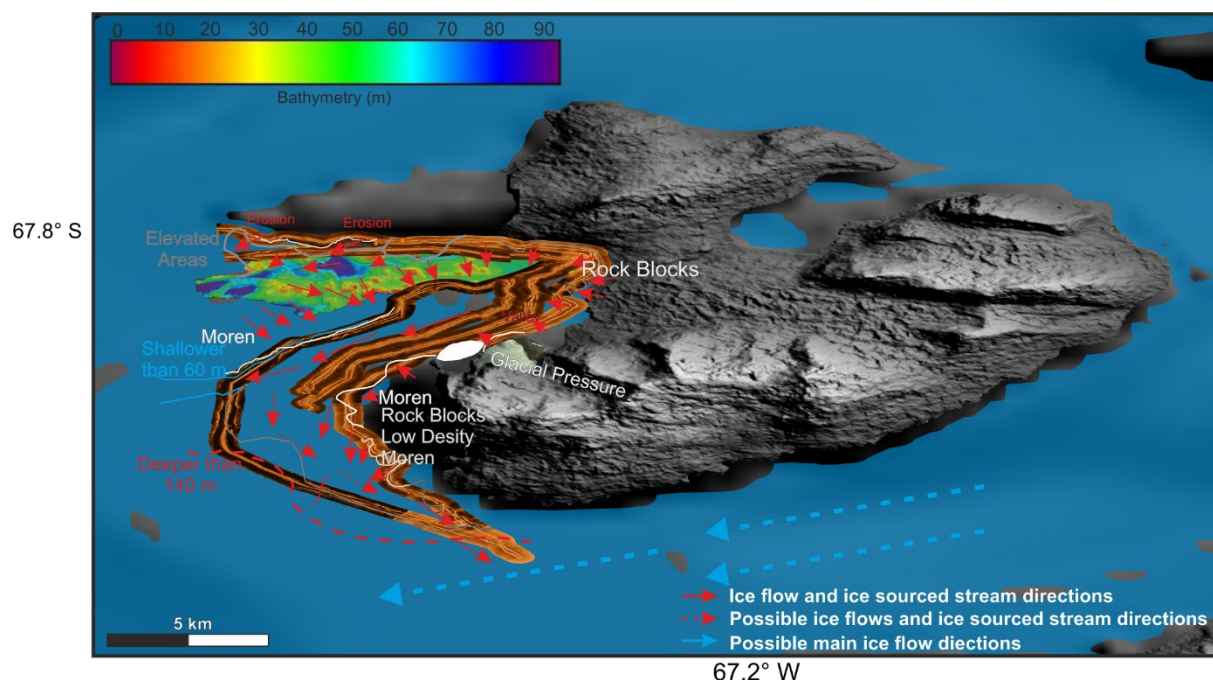
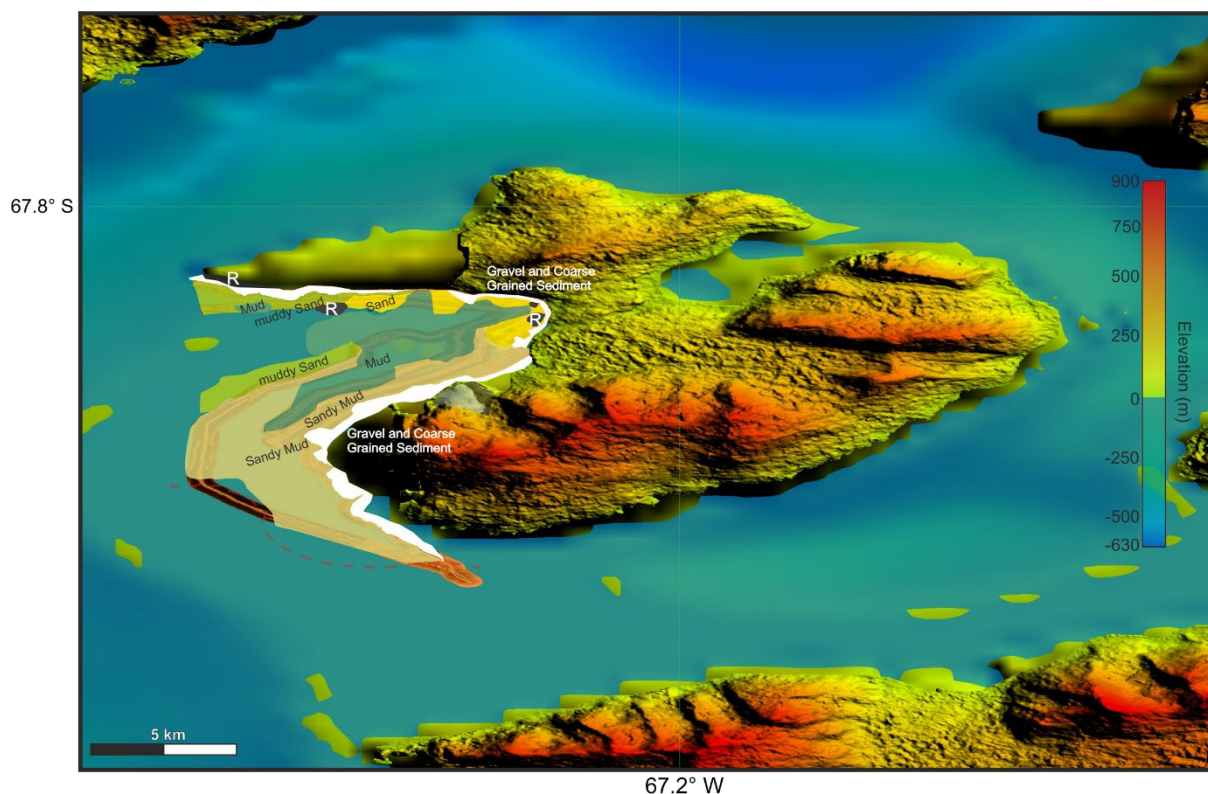


Fig 8. Ice flow and ice sourced stream direction for the study area



245 As a result, huge rock formations were found in the northwest, contrasting with the typically coarse-grained units found in nearby coastal regions. These rock blocks decrease in size towards the west, and in areas with a narrower distribution of grain sizes, randomly placed block rocks may be seen. In the research area between the northeastern and central northern regions, a sand-sized unit is observed above the coarse-grained sediments. Toward the south of this region, there is an abundance of low amplitude mud reflections, occasionally interrupted by high amplitude reflections, primarily extending from the north to the center of the study area. Medium to strong amplitude muddy sand units surround the western portion, while medium to low amplitude sandy mud units encircle the eastern and southern portions. Sandy mud units are relatively more widespread in the areas towards the south of the bay.

250 The presence of low amplitude mud-size sediments in the area, along with the appearance of the old shoreline in sections, suggests an unusual feature in the study area compared to the normal system. Typically, this area should consist of sand-muddy and sand grain size units. This anomaly indicates the presence of an earlier mechanism in this area, different from the normal system. It is hypothesized that this area, characterized as a paleo-lake, was likely formed during the subglacial phase, one of the glacial mechanisms. As the glaciers melted, the glacier-covered areas retreated towards the close shore (0–10 m), and the processes in the studied area were influenced by glacier-induced flow. It is assumed that this area was once covered by ice sheets, and the formation of the paleo-lake structure was a result of subglacial forces.



260

Fig 9. Sea floor sediment grain size distribution for the study area revealed from acoustic data and video captures



The side scan sonar data provides imaging of the recent seafloor, revealing areas of deposition and erosion that interact with the recent seafloor. These findings shed light on the plausible mechanisms mentioned earlier. Despite being the first data for the research area, there are very few studies in the literature that focus on nearshore glacial mechanisms. The vast areas covered by the research result in significant gaps in the definitions of nearshore deformation and sediment types. This study serves as a valuable reference in filling many of these gaps. However, further investigations are necessary to strengthen or enhance this study. One crucial aspect is examining the activity of the erosion and deformation zones identified in this study. Conducting high-resolution shallow seismic surveys on these sites can provide crucial information about sedimentary deposition in erosion areas or accumulation cuts in deposition areas. Additionally, a two-dimensional seismic section of the structure described as a paleolake can help calculate the thickness of sedimentary deposition.

Alternatively, conducting age studies on core samples collected in the basin or on the paleo coasts identified in this study can help date the mechanisms in the study area. These additional investigations will contribute to a deeper understanding of the processes shaping the nearshore areas in glacially active regions.

## 5 Conclusions

Nearshore deformations and deposition characteristics of Western Horseshoe Island were mapped using side scan sonar data and video ground-trothing. The erosional and morphological boundaries indicate that the seafloor, particularly up to a depth of 10 meters, has been predominantly influenced by ice melting streams during the recent past, indicating ice-margin and glacial marine phases. However, subglacial seafloor features, such as a paleolake, and paleoshoreline morphology were also identified in a limited area, indicating the presence of two-phase mechanisms in the study area.

The meltwater streams and ice flow directions generally trend towards the southern part of the study area, with the southern part of the island being deeper compared to the western part. Consequently, the ice-sourced mechanisms in the study area primarily trend towards the south and connect with the main ice-sourced mechanism in the south. Additionally, a western flow was also identified near the coast of the northern part of the study area.

The seafloor grain size is generally coarse-grained near the coast and becomes finer with increasing depth. However, towards the west, the grain size is relatively thicker, which is an anomaly from the normal circulation and indicates that ice melting dynamics are still active in the study area.

## Acknowledgement

The authors gratefully acknowledge the financial support of the Scientific and Technological Research Council of Turkey-TUBITAK (Project 122G264 ). We gratefully acknowledge that this study was carried out within the 8th Turkish Antarctic Expedition (TAE-8), under the auspices of the Presidency of the Republic of Türkiye, supported by the Ministry of Industry and Technology, and coordinated by TÜBİTAK MAM Polar Research Institute.

## Code/Data availability

Not applicable.



### Author contribution

295 Denizhan Vardar and Korhan Erturaç collected data. Denizhan Vardar made data processing. All authors worked on writings and figures of this manuscript

### Competing interests

Not applicable.

### 300 References

- Anandkrishnan, S., Alley, R.B.: Stagnation of ice stream C, West Antarctic by water piracy. *Geophys Res Lett* 24:265–268
- Barnhardt W. A., Kelley J T, Dickson S M, et al. 1998. Mapping the gulf of Maine with side-scan sonar: a new bottom-type classification for complex seafloors. *Journal of Coastal Research*, 14(2): 646–659
- Batchelor CL, Dowdeswell JA (2014) The physiography of high Arctic cross-shelf troughs. *Quat Sci Rev* 92:68–96
- 305 Batchelor CL, Dowdeswell JA, Ottesen D. (2018) Volcanic islands and seamounts. In *Submarine Geomorphology* (eds Micalef, A, Krastel, S and Savini, A), pp. 333–47. Cham: Springer International Publishing. doi: 10.1007/978-3-319-57852-1\_17.CrossRefGoogle ScholarOpenURL query
- Bentley CR (1987) Antarctic ice streams: a review. *J Geophys Res* 92:8843–885
- Bentley, M. J., Johnson, J. S., Hodgson, D. A., Dunai, T., Freeman, S. P. H. T., & Ó Cofaigh, C. (2011). Rapid deglaciation
- 310 of Marguerite Bay, Western Antarctic Peninsula in the Early Holocene. *Quaternary Science Reviews*, 30(23– 24), 3338–3349.
- Borgeld, J. C. , Hughes Clarke, J. E. , Goff, J. A. , Mayer, L. A. , & Curtis, J. A. (1999). Acoustic backscatter of the 1995 flood deposit on the Eel shelf. *Marine Geology*, 154(1–4) 197–210. [https://doi.org/ 10.1016/s0025-3227\(98\)00113-3](https://doi.org/10.1016/s0025-3227(98)00113-3)
- Briggs, K. B. , Williams, K. L. , Richardson, M. D. , & Jackson, D. R. (2001). Effects of Changing Roughness on Acoustic
- 315 Scattering: (1) Natural Changes
- Bull J M, Quinn R, Dix J K. 1998. Reflection coefficient calculation from marine high resolution seismic reflection (Chirp) data and application to an archaeological case study. *Marine Geophysical Researches*, 20(1): 1–11, doi: 10.1023/A:1004373106696
- Buscombe, D. (2017). Shallow water benthic imaging and substrate characterization using recreational-grade sidescan-sonar.
- 320 *Environmental Modelling & Software*, 89, 1–18. [https://doi.org/ 10.1016/j.envsoft.2016.12.003](https://doi.org/10.1016/j.envsoft.2016.12.003)
- Clark CD (1994) Large scale ice-moulded landforms and their glaciological significance. *Sed Geol* 91:253–268
- Collier J S, Brown C J. 2005. Correlation of sidescan backscatter with grain size distribution of surficial seabed sediments. *Marine Geology*, 214(4): 431–449, doi: 10.1016/j.margeo.2004.11.011



- Çiner, A., Yıldırım, C., Sarıkaya, M. A., Seong, Y. B., Byung, Y. Y. 2019. <sup>10</sup>Be cosmogenic dating of glacial erratic  
325 boulders on Horseshoe Island in western Antarctic Peninsula confirm the rapid deglaciation in Early Holocene. *Antarctic  
Science*, 31, 6, 319–331. doi:10.1017/S0954102019000439.
- Damuth JE (1978) Echo character of the Norwegian-Greenland Sea: relationship to Quaternary sedimentation. *Mar Geol*  
28:1–36
- Danielson, M. and Bart, P. J (2019) Topographic control on the post-LGM grounding zone locations of the West Antarctic  
330 Ice Sheet in the Whales Deep Basin, Eastern Ross Sea, *Mar. Geol.*, 407, 248260,  
<https://doi.org/10.1016/j.margeo.2018.11.001>, 2019.
- Danielson, M. and Bart, P. J (2024) The staggered retreat of grounded ice in the Ross Sea, Antarctica, since the Last Glacial  
Maximum (LGM The Cryosphere, 18, 1125–1138, 2024 <https://doi.org/10.5194/tc-18-1125-2024>
- Dowdeswell JA, Kenyon N, Elverhøi A et al (1996) Large-scale sedimentation on the glacier influenced Polar North Atlantic  
335 margins: long-range side-scan sonar evidence. *Geophys Res Lett* 23:3535–3538
- Dowdeswell JA, Siegert MJ (1999) Ice-sheet numerical modelling and marine geophysical measurements of glacier-derived  
sedimentation on the Eurasian Arctic continental margins. *Geol Soc Am Bull* 111:1080–1097
- Dowdeswell JA, Ó Cofaigh C, Taylor J et al (2002) On the architecture of high-latitude continental margins: the influence of  
ice-sheet and sea-ice processes in the Polar North Atlantic. In: Dowdeswell JA, Ó Cofaigh C (eds) *Glacier-influenced*  
340 *sedimentation on high-latitude continental margins*, Geological Society, London, Special Publication 203, pp 33–54
- Dowdeswell JA, Siegert MJ (1999) Ice-sheet numerical modelling and marine geophysical measurements of glacier-derived  
sedimentation on the Eurasian Arctic continental margins. *Geol Soc Am Bull* 111:1080–1097
- Dowdeswell JA, Ottesen D, Rise L (2006) Flow-switching and large-scale deposition by ice streams draining former ice  
sheets. *Geology* 34:313–316
- 345 Dowdeswell JA, Ó Cofaigh C, Pudsey CJ (2004) Continental slope morphology and sedimentary processes at the mouth of  
an Antarctic palaeo-ice stream. *Mar Geol* 204:203–214
- Dyke AS, Andrews JT, Clark PU et al (2002) The Laurentide and Innuitian ice sheets during the last glacial maximum. *Quat  
Sci Rev* 21:9–31
- Elverhøi A, Hooke RLeB, Solheim A (1998) Late Cenozoic erosion and sediment yield from the Svalbard-Barents Sea  
350 region: implications for understanding erosion of glacierised basins. *Quat Sci Rev* 17:209–242
- Fonseca, L. E. , Mayer, L. A. , Orange, D. , & Driscoll, N. (2002). The high-frequency backscattering angular response of  
gassy sediments: Model/data comparison from the Eel River Margin, California. University of New Hampshire Scholars  
Repository (University of New Hampshire at Manchester), 111(6), 2621– 2631. <https://doi.org/10.1121/1.1471911>
- Ferrini, V. L. , & Flood, R. D. (2006). The effects of fine-scale surface roughness and grain size on 300 kHz multibeam  
355 backscatter intensity in sandy marine sedimentary environments. *Marine Geology*, 228(1–4), 153–172.  
<https://doi.org/10.1016/j.margeo.2005.11.010>





- Goff J A, Kraft B J, Mayer L A, et al. 2004. Seabed characterization on the New Jersey middle and outer shelf: correlatability and spatial variability of seafloor sediment properties. *Marine Geology*, 209(1-4): 147–172, doi: 10.1016/j.margeo.2004.05.030
- 360 Grindlay N. 2009. Use of high-resolution sidescan sonar data to quantitatively map and monitor a mid-continental shelf hardbottom 23-mile site, Onslow bay, NC [dissertation]. Chapel Hill: University of North Carolina Wilmington
- Joughin I, Rignot E, Rosanova E et al (2003) Timing of recent accelerations of Pine Island Glacier, Antarctica. *Geophys Res Lett* 30:1706
- Larter RD, Graham ACG, Hillenbrand CD et al (2012) Late Quaternary grounded ice extent in the Filchner Trough, Weddell Sea, Antarctica: new marine geophysical evidence. *Quat Sci Rev* 53:111–122
- 365 MacAyeal DR (1993) Binge/purge oscillations of the Laurentide ice sheet as a cause of the North Atlantic’s Heinrich events. *Paleoceanography* 8:775–784
- Matthews, D. W. (1983). The geology of Horseshoe and Lagotellerie Islands, Marguerite Bay, Graham Land. *British Antarctic Survey Bulletin*, 52, 125–154.
- 370 Ottesen D, Dowdeswell JA, Rise L (2005) Submarine landforms and the reconstruction of fast-flowing ice streams within a large Quaternary ice sheet: the 2500-km-long Norwegian-Svalbard margin (57°–80°N). *Geol Soc Am Bull* 117:1033–1050
- Ó Cofaigh C, Pudsey CJ, Dowdeswell JA et al (2002) Evolution of subglacial bedforms along a paleo-ice stream, Antarctic Peninsula continental shelf. *Geophys Res Lett* 29:1199
- Ottesen D, Dowdeswell JA (2009) An inter-ice stream glaciated margin: submarine landforms and a geomorphic model based on marine-geophysical data from Svalbard. *Geol Soc Am Bull* 121:1647–1665
- 375 Ó Cofaigh, C., Dowdeswell, J. A., Evans, J., & Larter, R. D. (2008). Geological constraints on Antarctic palaeo-icestream retreat. *Earth Surface Processes and Landforms*, 33(4), 513–525.
- Ochyra, R., Smith, R. I. L., & Bednarek-Ochyra, H. (2008). *The illustrated Moss Flora of Antarctica* (p. 685). Cambridge: Cambridge University Press.
- 380 ÖZGAN Sinan, ALP Hakan, BAYAT Oğuz, VARDAR Denizhan. Acoustical imaging of the nearshore seafloor depositions and deformations, a key study for Western Istanbul, Türkiye[J]. *Acta Oceanologica Sinica*. doi: 10.1007/s13131-023-2197-3
- Pratomo D G, Cahyadi M N, Akbar K, et al. 2018. Analysis of seafloor sediment distribution using multibeam backscatter data. *MATEC Web of Conferences*, 177: 01026, doi: 10.1051/mateconf/201817701026
- Richardson MD, Briggs KB, Williams KL, Lyons AP, Jackson DR (2001) Effects of changing roughness on acoustic scattering: (2) anthropogenic change. In: Leighton TG, Heald GJ, Griffiths G, Griffiths HD (Eds), *Proceedings of the Institute of Acoustics*, vol. 23, Part 2, pp 343–390
- 385 Stewart, W. I. , Chu, D. , Malik, S. , Lerner, S. , & Singh, H. (1994). Quantitative seafloor characterization using a bathymetric sidescan sonar. *IEEE Journal of Oceanic Engineering*, 19(4), 599–610. <https://doi.org/10.1109/48.338396>
- Shipp SS, Anderson JB, Domack EW (1999) Late Pleistocene-Holocene retreat of the West Antarctic ice-sheet system in the Ross Sea: part 1—geophysical results. *Geol Soc Am Bull* 111:1486–1516
- 390



- Solheim A (1991) The depositional environment of surging sub-polar tidewater glaciers: a case study of the morphology, sedimentation and sediment properties in a surge-affected marine basin outside Nordaustlandet, northern Barents Sea. *Norsk Polarinstitutt Skrifter*, p 194
- Stokes CR, Clark CD (2001) Palaeo-ice streams. *Quat Sci Rev* 20:1437–1457
- 395 Stokes CR, Margold M, Clark CD et al (2016) Ice stream activity scaled to ice sheet volume during Laurentide ice sheet deglaciation. *Nature* 530:322–326
- Svendsen JI, Astakhov VI, Bolshiyakov D Yu et al (1999) Maximum extent of the Eurasian ice sheet in the Barents and Kara Sea region during the Weichselian. *Boreas* 28:234–242
- Tükenmez, E., Gülher, E., Kaya, Ö., Polat H.F., 2022. Bathymetric Analysis Of Lystad Bay, Horseshoe Island By Using High Resolution Multibeam Echosounder Data. *Journal of Naval Sciences and Engineering* 2022, Vol. 18, No. 2, pp. 281-303 *Oceanography and Hydrography*
- 400 Urgeles, R. , Locat, J. , Schmitt, T. , & Hughes, J. E. (2002). The July 1996 flood deposit in the Saguenay Fjord, Quebec, Canada: implications for sources of spatial and temporal backscatter variations. *Marine Geology*, 184
- Vorren TO, Laberg JS (1997) Trough mouth fans—palaeoclimate and ice-sheet monitors. *Quat Sci Rev* 16:865–881
- 405 Whillans IM, Bentley CR, van der Veen CJ (2001) Ice streams B and C. In: Alley RB, Bindschadler RA (eds) *The west Antarctic ice sheet: behavior and environment*, *Am Geophys Union Antarct Res Ser* 77:257–281
- Yıldırım, C.: Geomorphology of Horseshoe Island, Marguerite Bay, Antarctica, *Journal of Maps*, 16:2, 56-67, DOI: 10.1080/17445647.2019.1692700
- Smith, A. A., Carter, C., and Miller, B. B.: More test articles, *J. Adv. Res.*, 35, 13–28, doi:10.2345/67890, 2014.